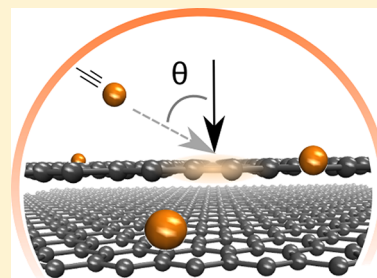


Atomistic Simulations of the Efficiencies of Ge and Pt Ion Implantation into Graphene

E. H. Åhlgren, A. Markevich, and E. Besley*[✉]

School of Chemistry, University of Nottingham, University Park, Nottingham NG7 2RD, United Kingdom

ABSTRACT: Recent success in the direct implantation of $^{74}\text{Ge}^+$ ion, the heaviest atomic impurity to date, into monolayer graphene presents a general question of the efficiency of low-energy ion implantation technique for heavy atoms. A comparative computational study, using classical molecular dynamics, of low-energy Ge and Pt ions implantation into single- and double-layer graphene is presented. It confirms that the highest probability for the perfect substitutional doping of single-layer graphene, i.e., direct implanting of ion into monovacancy, can be achieved 80 eV and it reaches the value of 64% for Ge ions directed at 45° angle to graphene plane and 21% for Pt ion beam perpendicular to graphene. Implantation efficiency is strongly dependent on the angle of ion beam. The sputtering yield of carbon atoms is found to be lower for double layer of graphene, which has better protective properties against low-energy ion irradiation damage than a single graphene layer. In double-layer graphene, incident ions traveling in the direction perpendicular to graphene can be trapped between the layers with the highest efficiency above or equal to 80% in the energy range of 40–90 eV for Ge ions and above 90% in the energy range of 40–70 eV for Pt ions. The energy range corresponding to the efficient trapping of ions in double-layer graphene is shifted toward higher energies upon tilting of the angle of incident ion beam.



INTRODUCTION

A search for new functionalities and applications of graphene has intensified since its discovery,^{1,2} often through chemical modification or altering its structure by implantation of new atomic species using low-energy ion beam irradiation.^{3–5} Metal-decorated graphene offers an attractive hybrid material for low-dimensional magnetic ordering and spintronics,⁶ with applications in electrocatalysis, fuel cells, energy production and storage, as well as electrochemical sensing.⁷ Typical values for the binding energy of metal adatom to pristine graphene range between 0.2 and 1.5 eV with the migration barrier of 0.2–0.8 eV,⁸ thus indicating its high mobility on graphene at room temperature. If metal atom is bound to a single or double vacancy in graphene, the migration barrier increases to 2.1–3.6 eV for a single vacancy and to 5 eV for a double vacancy leading to a stable trapping of metal in graphene structure. However, a single metal atom bound to larger vacancies and larger metal clusters attached to small vacancies are known to escape the vacancy traps at room temperature,⁹ and it is therefore important to find efficient ways for entrapment of single metal atoms in small vacancy defects to achieve a controllable atom-by-atom modification of graphene structure.

Previous studies show that a single metal atom can be trapped in graphene vacancies created by electron beam irradiation, notably assisted by the electron impacts in transmission electron microscopy experiments.^{9,10} Metal atom trapped in a single or double vacancy could also exhibit interesting dynamic behavior under electron beam as the values of the threshold energies for ejection of carbon atoms neighboring metal impurity are lower than those in pristine graphene. This has been illustrated recently by the case of Fe atom trapped in graphene vacancies.^{10,11} Wang et al.¹² used

ion bombardment (100–400 eV) to create vacancies in pristine graphene that were varying in size and then filled these vacancies with desired dopants. Low-energy ion implantation is another well-developed technique suitable for flexible manipulation of the structure and basic properties of materials using a variety of ion species, a wide range of implantation energies, and control over the dopant concentration through the ion beam flux. It has been shown to be effective for direct substitution of single carbon atoms in graphene with light atomic impurities, such as silicon,^{13–15} phosphorus,¹⁶ nitrogen and boron,^{17,18} and for intercalation of atoms between graphene layers.¹⁹

However, implantation of heavy atoms by ion irradiation is quite challenging in the case of two-dimensional materials, such as graphene, since only a narrow energy window will allow implantation: high enough to remove one or more target atoms yet low enough to stop the ion within the atomically thin structure. Recently, Tripathi et al. have demonstrated the possibility of direct implantation of $^{74}\text{Ge}^+$ ions into graphene.²⁰ In this work, the implantation efficiency for the case of 20 eV irradiation has been observed to be very low, only seven Ge impurities have been found directly in the lattice. The aim of current study is to systematically map the possibility of using direct implantation to introduce heavy atoms in graphene with low-energy ion beam irradiation. We use molecular dynamics simulations to investigate the aspects of trapping heavy Ge and Pt ions in single- and double-layer graphene. By varying irradiation parameters such as the ion

Received: July 29, 2018

Revised: October 16, 2018

Published: October 17, 2018

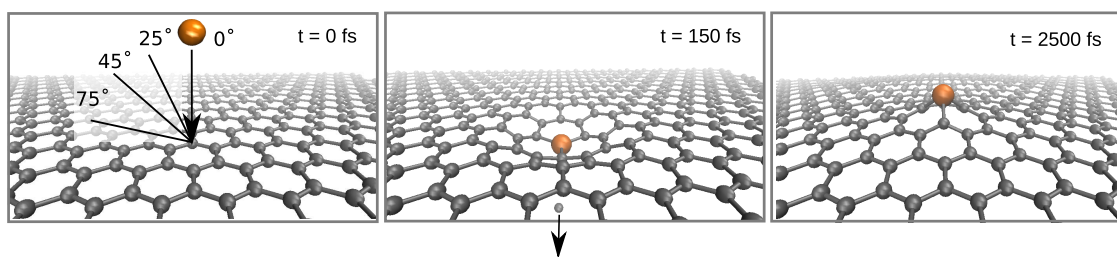


Figure 1. Snapshots taken from a molecular dynamics simulation presenting a Ge ion shot toward graphene replacing exactly one carbon atom in a direct implantation process.

energy and angle of incidence we establish the most favorable conditions for direct implantation.

■ COMPUTATIONAL METHODS

To study the implantation, we followed the same approach as in our earlier work on ion irradiation of both suspended^{3,21} and supported^{22–24} graphene. Only atomic interactions were taken into account, as for low energies the electronic stopping can be neglected to good approximation. Previous work also shows that with low charge states, the charge of the ion has only a minor role in the defect production in carbon nanostructures.²⁵ Regardless, we would like to point out that our method might miss some important chemical interactions between the ion and the nearest carbon atoms during the impact, and even more so, if the projectile has a high charge state. The simulations were performed with the classical molecular dynamics simulation PARCAS code.²⁶ We modeled graphene using a reactive bond order potential to describe interactions between the carbon atoms,²⁷ including a repulsive part²⁸ for small atomic separations. The potential gives a displacement threshold energy (the minimum kinetic energy required to sputter a carbon atom) of 22.59 eV, this is very close to the ones previously observed in theory calculations 22.2,²⁹ 23,³⁰ and 22.03 eV.³¹ The displacement thresholds given by theory are in the upper limit of the experimental ones due to minor thermal fluctuations and electronic effects that can lower the potential barrier.³⁰ During the ion impact, strong interactions between Ge/Pt and C, leading to the formation of chemical Ge/Pt–C bonds between the layers, are dominant over the van der Waals forces, and these interactions are modeled with the Tersoff potential³² for the Ge–C pair and the Albe potential³³ for the Pt–C interactions.

Each ion was shot toward a pristine target. At the start of simulation, the ion was placed 10 Å above the graphene plane. For each irradiation event, the coordinates of the impact point were randomly selected within an irreducible area of hexagonal lattice in the middle of the simulation cell ensuring statistically correct sampling. In the oblique irradiation angles, the x -coordinate of the ion was shifted to approximately 3 Å from the border of the cell to ensure that the ion impact does not cross over the cell boundary. After each irradiation event, the system was let to reach an energy minimum before it was analyzed. Simulation time was set to 2500 fs (single-layer, SL) and 3000 fs (double-layer, DL), with a time step dependent on the velocity of the fastest moving particle in the system. The simulation setups include SL graphene 20×18 supercell with 720 atoms and DL graphene with 17×20 supercell, including 1360 atoms with AB Bernal stacking and an interlayer distance of 3.35 Å after relaxation. Periodic boundary conditions were applied in x - and y -directions. During cell relaxation, the

temperature of the simulation cell was set to 0 K, and during the irradiation event the system was set in a quasimicrocanonical ensemble to avoid artefacts of the collision cascade. The cascade developed in a microcanonical ensemble (NVE) without scaling of the atom velocities. However, heat dissipation at the edges of the system was modeled with Berendsen thermostat,³⁴ including few atomic rows at the edges of the system to avoid energy transfer through the periodic boundaries and mimic energy dissipation into an infinite cell.

The energy of the projectile varied from 10 eV to 3 keV, and irradiation angles were 0 (perpendicular), 25, 45, and 75° off the normal of the surface, see Figure 1a, additional simulations were run with 70 and 75° to study the effect of large irradiation angles in trapping of the ion in DL graphene. We ran a total of 36 000 individual simulations, consisting of 150 simulations per each parameter set. On the basis of our previous experience in irradiation simulations, we are confident that this gives a representative distribution of defects produced in the target systems.

■ RESULTS AND DISCUSSION

We start analyzing the results by looking at the trapping efficiency of both ions at different irradiation angles and energies. We determine the final position and coordination number (number of nearest neighbors, cut-off 2.5 Å) for each ion. The implantation is then investigated more closely separating the “perfect” substitution events (exactly one carbon atom replaced by the ion) from the larger pool of events where the ion is placed in graphene accompanied by other defects, such as seven-membered rings and adatoms. We also determine the sputtering yield of carbon atoms (the average number of sputtered carbon atoms per incident ion) to estimate the damage produced to graphene. In the text, we use both expressions efficiency (0–100%) and probability (0–1).

Single-Layer Graphene. We start the discussion with SL graphene. Snapshots displaying the simulation setup with an example of direct implantation are shown in Figure 1. After the initial ion impact with the target, the ion can either be reflected from the surface, placed in graphene, or transmitted through it. The efficiency of placing the ion in graphene can be checked by simply counting the number of the ion’s nearest neighbors, i.e., the coordination number. The coordination number probabilities for Ge and Pt after the impact are shown in Figure 2 with snapshots of typical examples of the final atomic configurations seen in simulations. The highest efficiency found is 98% for Ge to be one-coordinated at 20 eV acceleration energy at 45° and 76% for Pt to be two-coordinated at 10 eV at perpendicular angle. These probabilities indicate a very high efficiency for implantation

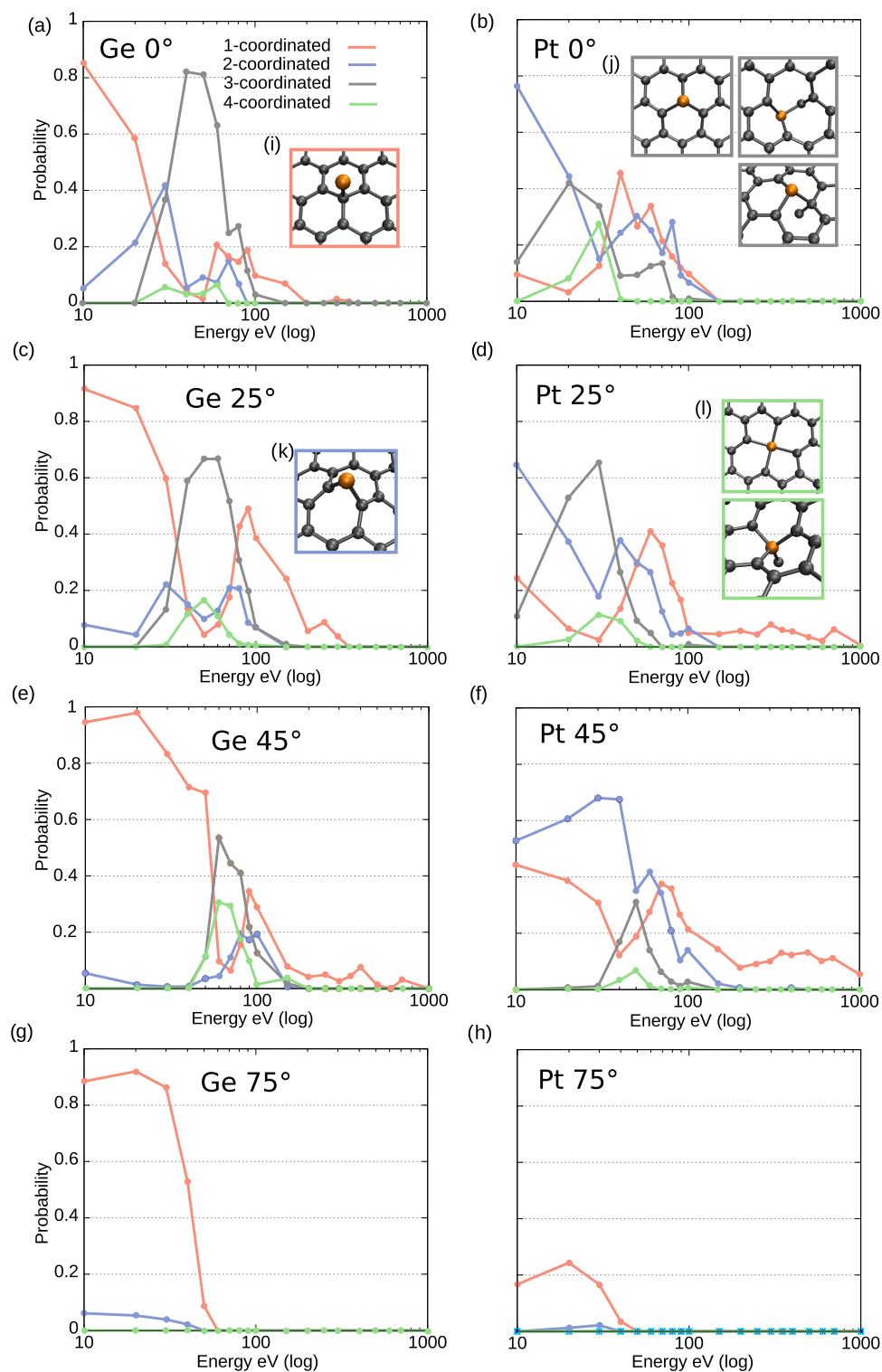


Figure 2. Probability of the ion to have different coordination numbers (number of nearest neighbors) after impact with single-layer graphene. Ge at (a) 0° (beam perpendicular to the surface), (c) 25° off the normal of graphene, (e) 45° and (g) 75° . Same for Pt (b) 0° , (d) 25° , (f) 45° and (h) 75° . The insets show examples of typical configurations for different coordination numbers seen in the simulations: (i) one-coordinated, (j) two-coordinated, (k) three-coordinated, and (l) four-coordinated. Note logarithmic scale on the X-axis.

with heavy ions when the right irradiation conditions are chosen. It is worth to note that after the impact, Ge and Pt atoms that are two-coordinated can in some cases be in a metastable configuration, and after further annealing at 500 K find a lower energy configuration and become three-coordinated. The probability for Ge ion to adopt three-

coordinated configuration decreases systematically when the angle is tilted off the normal, see the gray line in Figure 2a,c,e,g. For Pt ion, the highest efficiency to adopt three-coordinated configuration is seen at 25° off the normal.

We can also look at the implantation efficiency by taking into account only the perfect cases. The outcomes are then

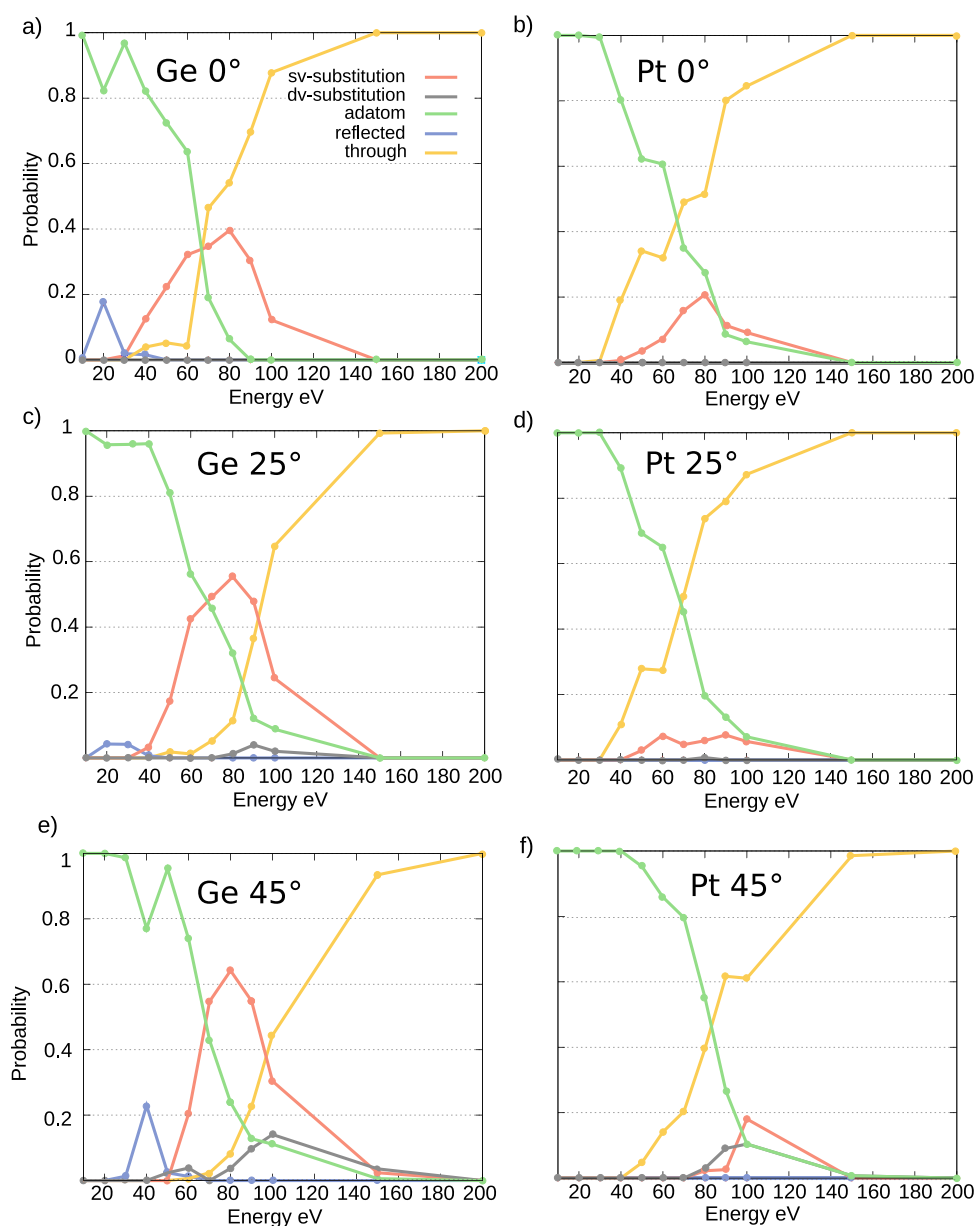


Figure 3. Probabilities for the ion to end up in the four main configurations after ion impact at different ion energies as discussed in the text. For Ge at (a) perpendicular, (c) 25° and (e) 45° toward the graphene plane. Same for Pt (b) perpendicular, (d) 25° and (f) 45°. At 75°, no direct implantation is seen for either ion.

divided in four main categories accordingly: (1) the ion knocks out exactly one carbon atom that is sputtered and takes its place in the lattice (single vacancy “sv”-substitution), (2) the ion detaches exactly two carbon atoms and takes their place in the lattice (double vacancy “dv”-substitution), (3) adatom (the ion settles on top of the lattice, but no carbon atoms are sputtered), and (4) the ion goes through the sheet and ends up in vacuum below. The probabilities are plotted in Figure 3.

The maximum efficiency of perfect sv-substitution is 64% at 80 eV and 45° for Ge and 21% at 80 eV for Pt at perpendicular angle of incidence. At these energies, Ge has enough energy to sputter one carbon atom and take its place in the lattice, but not enough energy to travel through graphene, the probability being only 0.08. Therefore, the efficiency of perfect sv-substitution is still high for Ge. The corresponding sputtering yield for Ge is seen to be 0.80. This is about one sixth higher than the sv-substitution efficiency, indicating that in some

events more than one carbon atom is sputtered during the impact due to the 45° inclination of the beam. Some of these events lead to dv-substitution, the efficiency being 4% at 80 eV.

On the other hand, heavier Pt has about 3 times lower maximum efficiency for perfect sv-substitution, only 21%, than Ge. This can be explained by the high probability of 0.52 for the ion to pass through graphene at this energy. Thus, the energy window in which perfect sv-substitution can be achieved for the heavier ion is found to get very narrow. The sputtering yield at the energy corresponding to the maximum sv-substitution efficiency is exactly the same as the ion’s sv-substitution efficiency, meaning that every event that leads to sputtering of carbon will lead to sv-substitution. Keeping in mind that the overall efficiency of perfect sv-substitution for Pt is low, a better chance of implantation for the ion is achieved at the very low energies where the peak efficiency was found to be 76% at 10 eV for the ion to be two-

Table 1. Maximum Probabilities of Implanting Ge and Pt Atoms in Single Vacancy (sv-Substitution) and Double Vacancy (dv-Substitution), and the Highest Probabilities for the Atom to be One-, Two-, Three-, and Four-Coordinated in Single-Layer Graphene^a

ion	0°	energy eV	25°	energy eV	45°	energy eV	75°	energy eV
sv-substitution	0.40	80	0.55	80	0.64	80	0.0	
dv-substitution	0.0		0.04	90	0.14	100	0.0	
1-coordinated	0.85	10	0.92	10	0.98	20	0.92	20
2-coordinated	0.42	30	0.22	30	0.19	80	0.06	10
3-coordinated	0.82	40	0.67	50, 60	0.54	60	0.0	
4-coordinated	0.07	60	0.17	50	0.31	60	0.0	
ion Pt	0°	energy eV	25°	energy eV	45°	energy eV	75°	energy eV
sv-substitution	0.21	80	0.08	90	0.18	100	0.0	
dv-substitution	0.0		0.01	80	0.10	100	0.0	
1-coordinated	0.45	40	0.41	60	0.44	10	0.24	20
2-coordinated	0.76	10	0.65	10	0.68	30	0.02	30
3-coordinated	0.42	20	0.66	30	0.31	50	0.0	
4-coordinated	0.28	30	0.11	30	0.07	50	0.0	

^aThe corresponding energy is given after each probability for all irradiation angles 0, 25, 45, and 75° off the normal of graphene plane.

coordinated, with another peak of 42% of three-coordinated atoms at 20 eV, see Figure 2c. For both ions, the direct implantation at low energies is most heavily restricted by the low sputtering yield of carbon atoms, see Figure 6. No implantation is seen when the beam is directed at 75° off the normal of graphene. At this angle, the ion is either placed on top of graphene as an adatom at low energies (up to about 50 eV for Ge and about 100 eV for Pt, after which the efficiency drops below 10%), or is reflected back.

In a pure head-on collision, the threshold energy for the formation of a perfect sv-substitution is found to be 28.30 eV for Ge and 34.61 eV for Pt. Recent density functional theory-based calculations by Tripathi et al.²⁰ report an energy range of 26–42 eV leading to a perfect sv-substitution for Ge in a pure head-on collision. The threshold matches reasonably well to the threshold found in our simulations, being slightly lower. In our simulations, the C–C bonds after the impact are stretched to 1.46–1.51 Å compared to 1.42 Å in pristine graphene. The Ge–C bonds are 1.78 Å, about 6% shorter than 1.89 Å in the configuration reported by Tripathi, thus implying that Ge atom typically sits deeper in the vacancy and it is closer to the sp³ carbons. The Pt–C bonds are 1.97 Å, only slightly longer than the 1.93 Å reported by Krasheninnikov.⁸

A perfect head-on collision is a rare event, which is taken into account in our simulations by varying the impact point, and hence the maximum substitution probability is found at higher energies than the threshold energy. At an energy slightly lower than the threshold, the ion can still take the place of carbon atom in graphene, but the transferred kinetic energy is not enough to lead to sputtering and the carbon stays in the lattice as an adatom, see an example in Figure 2g, the two configurations on the right hand side of the panel.

dv-Substitution is seen only at oblique irradiation angle, the maximum probability being about 0.14 for Ge and 0.10 for Pt, both at 100 eV and angle of 45°. The atom is required to sputter two carbon atoms during a single impact, which is more probable when the atom is coming in an angle than perpendicularly toward graphene. Sputtering yield at 100 eV at 45° is double that of 0° for Ge and also higher for Pt at an oblique angle. All of the maximum probabilities for vacancy substitutions as well as coordination numbers for both ions are gathered in Table 1.

In the case of substitutional doping, annealing of the structure after irradiation has been reported to substantially decrease the number of defects on carbon nanotubes, though preserving the substitutional atoms.³⁵ Same method could be used to rid graphene of any additional defects and adatoms after the ion implantation. Also, additional irradiation at a lower energy than that of the maximum vacancy-trapping probability would increase the amount of mobile Ge and Pt adatoms on the structure that could then combine with any existing vacancy defects even at room temperature.

A comparison, including previously reported computational work, on the efficiency of direct ion implantation into single vacancy in graphene (sv-substitution) has been made in Figure 4. It includes the following ions: N,^{3,36} B,^{3,36} O,³⁷ Si,³⁸ Ge,²⁰ Pt, and Au.³⁷ The energy of the ion directed perpendicularly toward graphene is shown as a function of the ion mass. The

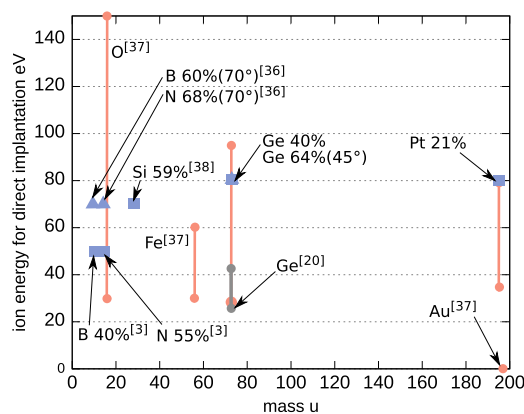


Figure 4. Efficiency of direct implantation into single vacancy in SL graphene shown for different ions. The blue squares indicate the energy corresponding to the highest efficiency of implantation as predicted by molecular dynamics simulations for irradiation angle perpendicular to graphene; the blue triangles indicate the values for off-normal irradiation angle given in round brackets; the red circles indicate the range between minimum and maximum energies leading to sv-substitution in a head-on collision as predicted by molecular dynamics simulations; the gray circles indicate the range between minimum and maximum energies leading to sv-substitution in a head-on collision predicted by density functional theory. References are given in the square brackets.

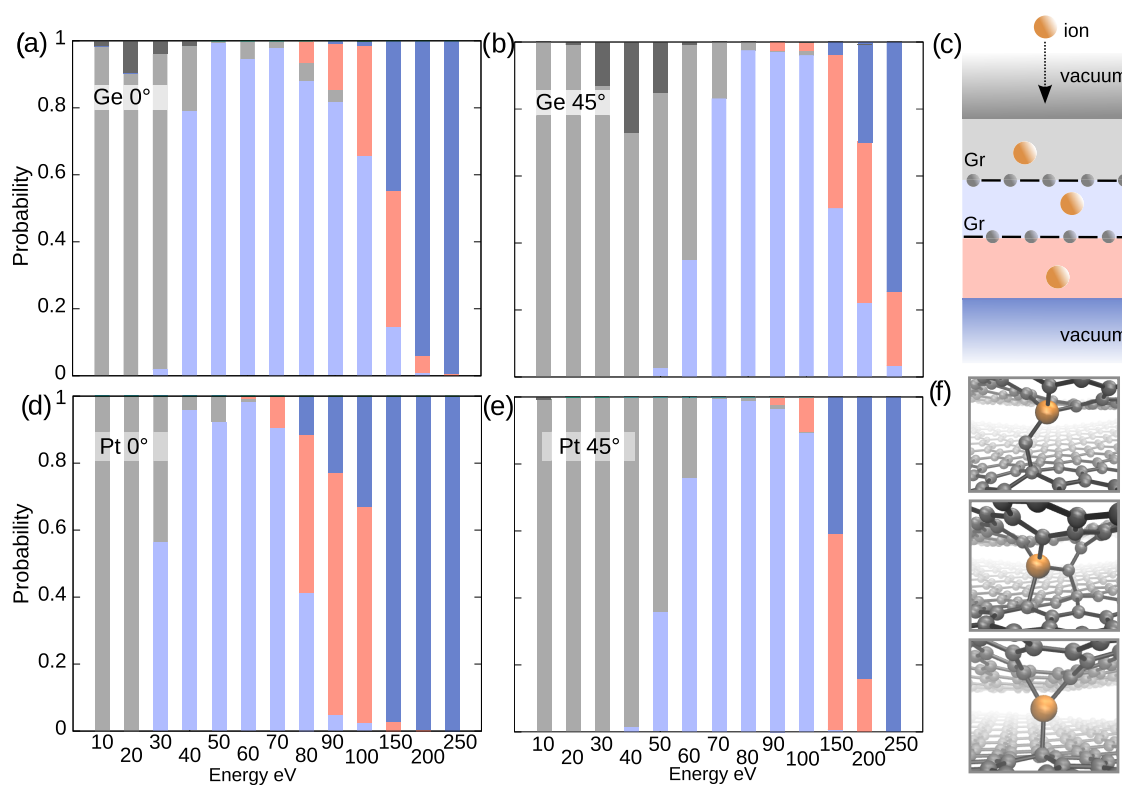


Figure 5. Histogram with probabilities of Ge and Pt to be found at different areas of double-layer graphene according to the atom's position after impact. Color coded according to (c): dark gray (vacuum, atom is reflected back), light gray (atom is trapped in the first layer), light blue (the atom is trapped between the layers), light red (atom is trapped in the second layer), and dark blue (vacuum, atom goes through both layers). (a) Ge at 0° , (b) Ge at 45° , (d) Pt at 0° , and (e) Pt at 45° . (f) Examples of typical configurations of Ge and Pt trapped between two graphene layers seen in the simulations.

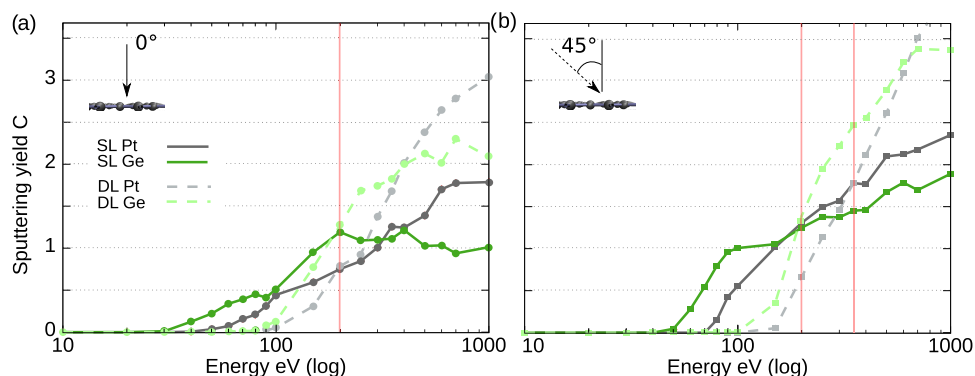


Figure 6. Sputtering yield of carbon atoms plotted as a function of the ion energy (logarithmic scale). The continuous lines describe the sputtering from single-layer graphene (SL), and the dotted lines sputtering from double-layer graphene (DL). The green color indicates Ge and gray Pt. The red vertical lines represent the energies at which the sputtering yield from DL graphene exceeds the one from SL graphene.

blue rectangles indicate the energy corresponding to the highest efficiency of *sv*-substitution as obtained from molecular dynamics simulations, with the efficiency indicated as percentage. For B, N, and Ge, the efficiency of implantation has been seen to improve at an angle off-normal to graphene; these values are shown in the blue triangles with the corresponding angle given in the round brackets.

The red circles joined with the lines indicate the energy range between the minimum and maximum energies leading to implantation in a direct head-on collision reported in molecular dynamics simulations. For Pt ion, the highest efficiency of pure *sv*-substitution (blue rectangle) is seen at the high-end of the head-on collision range (red) due to the low

sputtering yield of carbon at lower energies. The gray circles joined with a line indicate the energy range between the minimum and maximum energies at which implantation takes place in a direct head-on collision reported for Ge using density functional theory calculations.²⁰ The corresponding energy range from molecular dynamics reaches somewhat higher energies. For Au, no direct implantation in a head-on collision occurs, although the adatom configuration has been reported at very low energies (20 eV). This indicates that heavy atoms that cannot be implanted by direct *sv*-substitution can be introduced into the structure indirectly through adatom implantation. These mobile adatoms recombine with defects that can be created during irradiation with slightly higher

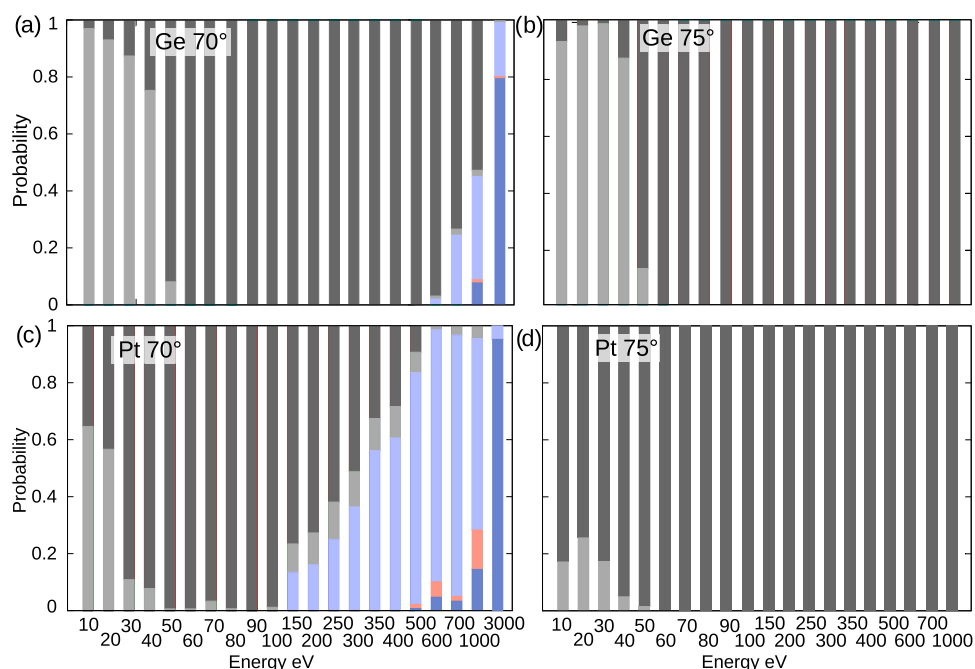


Figure 7. Histogram displaying a decrease in the trapping of Ge and Pt atoms in DL graphene as the irradiation angle is increased from 70 to 75°. The probability for the atom to be found at different areas of the DL system is mapped with the same color coding as in Figure 5. (a) Ge at 70°, (b) Ge at 75°, (c) Pt at 70°, (d) Pt at 75°.

energies, for which the sputtering yield of carbon is greater than zero.

Double-Layer Graphene. The ion can be implanted in either the first or the second layer or trapped between the two layers in a DL system. We analyzed the location of the atom by dividing the system into five layers: the topmost and lowest representing vacuum above and below the system, and three layers between consisting of the two graphene sheets and their interlayer area, see Figure 5c indicating the layers. The atom is regarded trapped when it is positioned between the two layers after impact, including cases where the atom bonds with the atoms in either layer and is bent toward the area between the layers, see examples in Figure 5f. The probabilities for the atom to be found in each of these layers are shown in Figure 5a,b,d,e.

The highest efficiency to trap Ge between two graphene layers is found to be above or equal to 80% at energies between 40–90 eV, and above 90% between 40–70 eV for Pt at perpendicular angle of irradiation, see the light blue area indicated in Figure 5a,d. The corresponding coordination number at these energies shows a clear peak for four-coordinated atoms with maximum of 71% at 60 eV for Ge and 59% at 40 eV for Pt. Lower irradiation energy results in the atom implanted in the first layer, displayed as the light gray area in Figure 5a,d. The sputtering yield of carbon below 50 eV is 0 (and stays less than 0.1 up to 90 eV for both ions). Sputtering is prevented by the second layer that acts as a protective substrate, reducing sputtering at the low energies, see Figure 6 for the sputtering yields. Similar behavior has been reported for ion irradiation of SL graphene on metal substrate at low energies.²²

With increasing irradiation angle, at 45°, the ion needs more energy to pass through the first layer and the trapping shifts to higher energies, see Figure 5b,e. The implantation in the first layer (light gray area) is dominant up to 60 eV for Ge and 50 eV for Pt, only reduced somewhat for Ge between 30 and 50 eV by atoms reflected back from the surface. The highest

probability for trapping at 45° is seen at 70–100 eV for Ge and 60–100 eV for Pt. At energies higher than these, the probability for Ge and Pt to pass through both layers starts to increase. Trapping of atoms between graphene and a substrate's surface due to ion irradiation has previously been reported for noble gas ions.²⁴

The two systems SL and DL graphene have a principal difference. The SL represents a freestanding system and the DL system can be considered as SL on an ultimately thin substrate, another single layer. The irradiation-induced sputtering yield of carbon atoms is lower from DL than from SL at low energies, and after a certain threshold energy the trend is reversed. The threshold energy is 200 eV for Ge and Pt with perpendicular irradiation angle and Ge at 45°. The threshold is 350 eV for Pt at 45°, see Figure 6 with the vertical red lines indicating the threshold energies. For even larger angles of 75°, the sputtering yield from SL does not exceed that of DL within the range of energies included in this study. At energies lower than the threshold energy, the second layer acts as a protective layer and decreases the sputtering. Similar protective effect is reported for graphene on bulk substrate at energies below 1 keV.²²

Finally, we studied the effect of high irradiation angles for trapping in DL graphene. We chose two angles, 70 and 75°, from the normal of graphene. Within the change of 5° in the incident angle, a drastic decrease is seen in the trapping of Ge and Pt atoms, indicating the importance of choosing a correct beam angle. Figure 7 displays histograms of the positions of Ge and Pt atoms after the impact, the color coding following the one in Figure 5. Ge ion can penetrate the first layer at 70° with acceleration energy of 600 eV, the corresponding value being 150 eV for Pt. The ion loses most of its kinetic energy while penetrating the first layer and is trapped in the interface. At 75°, neither ion is seen to penetrate the first layer up to the highest studied energy of 1 keV. At this angle, the ions are

either implanted in the first layer with energies up to 50 eV or reflected back from the first layer at energies higher than that.

CONCLUSIONS

Implantation of Ge and Pt atoms in single- and double-layer graphene using low-energy ion irradiation was studied by molecular dynamics simulations. The results show that implantation is possible through a single-step process in which the ion directly replaces a carbon atom in the lattice when the ion energy and angle are chosen carefully. The highest efficiency of perfect sv-substitutional doping in single-layer graphene is achieved for Ge and Pt ions accelerated at 80 eV reaching the value of 64% for Ge directed at 45° angle to graphene plane and 21% for Pt ion beam perpendicular to graphene. By taking into account cases, in which the ion is implanted into the lattice, including configurations consisting of additional defects, such as seven-membered rings and adatoms, the highest efficiency for implantation can be as high as 98% for Ge at 20 eV and 76% for Pt at 10 eV, both at perpendicular irradiation angle. In general, Ge was found to have a higher efficiency to be implanted than Pt at the studied energies.

Irradiation of double-layer graphene with Ge and Pt ions is shown to lead to trapping of the ions between the layers with the maximum efficiency above or equal to 80% for Ge at acceleration energies between 40 and 90 eV and above 90% between acceleration energies of 40 and 70 eV for Pt, both at perpendicular ion beam angle. Tilting the beam by 45° shifts the probabilities of trapping to higher energies. The sputtering yield of carbon atoms is found to be higher for single layer than double-layer graphene below a threshold energy of 200 or 350 eV depending on the ion species and angle of incidence. This indicates protective properties against low-energy ion irradiation damage for double-layer structures.

By carefully choosing the correct irradiation conditions, our results predict that low-energy ion irradiation could be used to directly implant a large variety of possible atomic species from light to heavy in two-dimensional materials, opening a door to new applications through chemical and structural modifications.

AUTHOR INFORMATION

Corresponding Author

*E-mail: elena.besley@nottingham.ac.uk

ORCID

E. Besley: 0000-0002-9910-7603

Notes

The authors declare no competing financial interest.

ACKNOWLEDGMENTS

E.B. acknowledges funding from the European Research Council under the European Union's Seventh Framework Programme (FP7)/ERC grant agreement No. 307755-FIN. Computational simulations were performed at the High Performance Computing Facility at the University of Nottingham. We acknowledge the use of Athena at HPC Midlands+, which was funded by the EPSRC on grant EP/P020232/1 as part of the HPC Midlands+ consortium.

REFERENCES

- (1) Novoselov, K. S.; Geim, A. K.; Morozov, S. V.; Jiang, D.; Zhang, Y.; Dubonos, S. V.; Grigorieva, I. V.; Firsov, A. A. Electric Field Effect in Atomically Thin Carbon Films. *Science* **2004**, *306*, 666–669.
- (2) Novoselov, K. S.; Morozov, S. V.; Mohinddin, T. M. G.; Ponomarenko, L. A.; Elias, D. C.; Yang, R.; Barbolina, I.; Blake, P.; Booth, T. J.; Jiang, D.; Giesbers, J.; Hill, E. W.; Geim, A. K. Electronic Properties of Graphene. *Phys. Status Solidi B* **2007**, *244*, 4106–4111.
- (3) Åhlgren, E. H.; Kotakoski, J.; Krasheninnikov, A. V. Atomistic Simulations of the Implantation of Low-Energy Boron and Nitrogen Ions into Graphene. *Phys. Rev. B* **2011**, *83*, No. 115424.
- (4) Bangert, U.; Pierce, W.; Kepaptsoglou, D. M.; Ramasse, Q.; Zan, R.; Gass, M. H.; den Berg, J. A. V.; Boothroyd, C. B.; Amani, J.; Hofsäss, H. Ion Implantation of Graphene - Toward IC Compatible Technologies. *Nano Lett.* **2013**, *13*, 4902–4907.
- (5) Kotakoski, J.; Krasheninnikov, A. V.; Ma, Y.; Foster, A. S.; Nordlund, K.; Nieminen, R. M. B and N Ion Implantation into Carbon Nanotubes: Insight from Atomistic Simulations. *Phys. Rev. B* **2005**, *71*, No. 205408.
- (6) Yazyev, O. V. Emergence of Magnetism in Graphene Materials and Nanostructures. *Rep. Prog. Phys.* **2010**, *73*, No. 056501.
- (7) Giovanni, M.; Poh, H. L.; Ambrosi, A.; Zhao, G.; Sofer, Z.; Šaněk, F.; Khezri, B.; Webster, R. D.; Pumera, M. Noble Metal (Pd, Ru, Rh, Pt, Au, Ag) Doped Graphene Hybrids for Electrocatalysis. *Nanoscale* **2012**, *4*, 5002–5008.
- (8) Krasheninnikov, A. V.; Lehtinen, P. O.; Foster, A. S.; Pyykkö, P.; Nieminen, R. M. Embedding Transition-Metal Atoms in Graphene: Structure, Bonding, and Magnetism. *Phys. Rev. Lett.* **2009**, *102*, No. 126807.
- (9) Rodríguez-Manzo, J. A.; Cretu, O.; Banhart, F. Trapping of Metal Atoms in Vacancies of Carbon Nanotubes and Graphene. *ACS Nano* **2010**, *4*, 3422–3428.
- (10) Robertson, A. W.; Montanari, B.; He, K.; Kim, J.; Allen, C. S.; Wu, Y. A.; Olivier, J.; Neethling, J.; Harrison, N.; Kirkland, A. I.; Warner, J. H. Dynamics of Single Fe Atoms in Graphene Vacancies. *Nano Lett.* **2013**, *13*, 1468–1475.
- (11) Markevich, A. V.; Baldoni, M.; Warner, J. H.; Kirkland, A. I.; Besley, E. Dynamic Behaviour of Single Fe Atoms Embedded in Graphene. *J. Phys. Chem. C* **2016**, *120*, 21998–22003.
- (12) Wang, H.; Wang, Q.; Cheng, Y.; Li, K.; Yao, Y.; Zhang, Q.; Dong, C.; Wang, P.; Schwingschlögl, U.; Yang, W.; Zhang, X. X. Doping Monolayer Graphene with Single Atom Substitutions. *Nano Lett.* **2012**, *12*, 141–144.
- (13) Zhou, W.; Kapetanakis, M. D.; Prange, M. P.; Pantelides, S. T.; Pennycook, S. T.; Idrobo, J.-C. Direct Determination of the Chemical Bonding of Individual Impurities in Graphene. *Phys. Rev. Lett.* **2012**, *109*, No. 206803.
- (14) Ramasse, Q. M.; Seabourne, C. R.; Kepaptsoglou, D.-M.; Zan, R.; Bangert, U.; Scott, A. J. Probing the Bonding and Electronic Structure of Single Atom Dopants in Graphene with Electron Energy Loss Spectroscopy. *Nano Lett.* **2013**, *13*, 4989–4885.
- (15) Susi, T.; Meyer, J. C.; Kotakoski, J. Manipulating Low-Dimensional Materials Down to the Level of Single Atoms with Electron Irradiation. *Ultramicroscopy* **2017**, *180*, 163–172.
- (16) Susi, T.; Hardcastle, T. P.; Hofsäss, H.; Mittelberger, A.; Pennycook, T. J.; Mangler, C.; Drummond-Brydson, R.; Scott, A. J.; Meyer, J. C.; Kotakoski, J. Single-Atom Spectroscopy of Phosphorus Dopants Implanted into Graphene. *2D Mater.* **2017**, *4*, No. 021013.
- (17) Bangert, U.; Stewart, A.; O'Connell, E.; Courtney, E.; Ramasse, Q.; Kepaptsoglou, D.; Hofsäss, H.; Amani, J.; Tu, J.-S.; Kardynal, B. Ion-Beam Modification of 2-D Materials - Single Implant Atom Analysis via Annular Dark-Field Electron Microscopy. *Ultramicroscopy* **2017**, *176*, 31–36.
- (18) Kepaptsoglou, D.; Hardcastle, T. P.; Seabourne, C. R.; Bangert, U.; Zan, R.; Amani, J. A.; Hofsäss, H.; Nicholis, R. J.; Brydson, R. M. D.; Scott, A. J.; Ramasse, Q. M. Electronic Structure Modification of Ion Implanted Graphene: The Spectroscopic Signatures of p- and n-Type Doping. *ACS Nano* **2015**, *9*, 11398–11407.

- (19) Zhao, S.; Xue, J. Tuning the Band Gap of Bilayer Graphene by Ion Implantation: Insight from Computational Studies. *Phys. Rev. B* **2012**, *86*, No. 165428.
- (20) Tripathi, M.; Markevich, A.; Böttger, R.; Facsko, S.; Besley, E.; Kotakoski, J.; Susi, T. Implanting Germanium into Graphene. *ACS Nano* **2018**, *12*, 4641–4647.
- (21) Åhlgren, E. H.; Kotakoski, J.; Lehtinen, O.; Krasheninnikov, A. V. Ion Irradiation Tolerance of Graphene as Studied by Atomistic Simulations. *Appl. Phys. Lett.* **2012**, *100*, No. 233108.
- (22) Åhlgren, E. H.; Hämmäläinen, S. K.; Lehtinen, O.; Liljeroth, P.; Kotakoski, J. Structural Manipulation of Graphene/Metal Interface with Ar⁺ Irradiation. *Phys. Rev. B* **2013**, *88*, No. 155419.
- (23) Herbig, C.; Åhlgren, E. H.; Schröder, U. A.; Martínez-Galera, A. J.; Arman, M. A.; Kotakoski, J.; Knudsen, J.; Krasheninnikov, A. V.; Michely, T. Xe Irradiation of Graphene on Ir(111): From Trapping to Blistering. *Phys. Rev. B* **2015**, *92*, No. 085429.
- (24) Herbig, C.; Åhlgren, E. H.; Michely, T. Blister-Free Ion Beam Patterning of Supported Graphene. *Nanotechnology* **2017**, *28*, No. 055304.
- (25) Krasheninnikov, A. V.; Nordlund, K. Ion and Electron Irradiation-Induced Effects in Nanostructured Materials. *J. Appl. Phys.* **2010**, *107*, No. 071301.
- (26) Nordlund, K.; Ghaly, M.; Averback, R.; Cartula, M.; de la Rubia, T. D.; Tarus, J. Defect Production in Collision Cascades in Elemental Semiconductors and fcc Metals. *Phys. Rev. B* **1998**, *57*, 7556–7570.
- (27) Brenner, D. W.; Shenderova, O. A.; Harrison, J. A.; Stuart, S. J.; Ni, B.; Sinnott, S. B. A Second-Generation Reactive Empirical Bond Order (REBO) Potential Energy Expression for Hydrocarbons. *J. Phys.: Condens. Matter* **2002**, *14*, 783–802.
- (28) *The Stopping and Range of Ions in Matter*; Ziegler, J. F.; Biersack, J. P.; Littmark, U., Eds.; Pergamon: New York, 1985.
- (29) Krasheninnikov, A. V.; Banhart, F.; Li, J. X.; Foster, A. S.; Nieminen, R. M. Stability of Carbon Nanotubes Under Electron Irradiation: Role of Tube Diameter and Chirality. *Phys. Rev. B* **2005**, *72*, No. 125428.
- (30) Zobelli, A.; Gloter, A.; Ewels, C. P.; Seifert, G.; Colliex, C. Electron Knock-On Cross Section of Carbon and Boron Nitride Nanotubes. *Phys. Rev. B* **2007**, *75*, No. 245402.
- (31) Kotakoski, J.; Jin, C. H.; Lehtinen, O.; Suenaga, K.; Krasheninnikov, A. V. Electron Knock-On Damage in Hexagonal Boron Nitride Monolayers. *Phys. Rev. B* **2010**, *82*, No. 113404.
- (32) Tersoff, J. Modeling Solid-State Chemistry: Interatomic Potentials for Multicomponent Systems. *Phys. Rev. B* **1989**, *39*, No. 5566.
- (33) Albe, K.; Nordlund, K.; Averback, R. S. Modeling the Metal-Semiconductor Interaction: Analytical Bond-Order Potential for Platinum-Carbon. *Phys. Rev. B* **2002**, *65*, No. 195124.
- (34) Berendsen, H. J. C.; Postma, J. P. M.; van Gunsteren, W. F.; DiNola, A.; Haak, J. R. Molecular Dynamics with Coupling to an External Bath. *J. Chem. Phys.* **1984**, *81*, 3684.
- (35) Xu, F.; Minniti, M.; Barone, P.; Sindona, A.; Bonanno, A.; Oliva, A. Nitrogen Doping of Single Walled Carbon Nanotubes by Low Energy N₂⁺ Ion Implantation. *Carbon* **2008**, *46*, 1489–1496.
- (36) Bai, Z.; Zhang, L.; Liu, L. Improving Low-Energy Boron/Nitrogen Ion Implantation in Graphene by Ion Bombardment at Oblique Angles. *Nanoscale* **2016**, *8*, 8761–8772.
- (37) Liu, X. Y.; Wang, F. C.; Park, H. S.; Wu, H. A. Defecting Controllability of Bombarding Graphene with Different Energetic Atoms via Reactive Force Field Model. *J. Appl. Phys.* **2013**, *114*, No. 054313.
- (38) Li, W.; Xue, J. Ion Implantation of Low Energy Si Into Graphene: Insight from Computational Studies. *RSC Adv.* **2015**, *5*, 99920.